On Edge Waves Occurring in Forming a Circular Channel Section with Side Flanges by Cold Roll Forming

By

Jun-ichi KOKADO* and Yoshitomi ONODA**

(Received December 22, 1976)

The mechanism of the occurrence of edge waves occurring in forming a strip into a circular channel section with side flanges by a single stand roll forming has been experimentally investigated from the relations between the forming conditions and the membrane strains and stresses produced during passage through the rolls.

It was found that the product after roll forming was contracted longitudinally at the center of the circular channel section, and elongated at the shoulder portion, and had both conditions (contraction, elongation) at the edge portion according to the forming conditions. It was also found that the transverse distribution zone of both the positive longitudinal residual membrane strain and stress in the flange ranged from the shoulder portion to beyond the middle point of the flange in the absence of edge waves. In this experiment, when the maximum value of the longitudinal compressive membrane strain at the center of the circular channel section was over 0.4%, without fail, edge waves occurred for the thickness of the strip over 0.8 mm.

Finally, it was confirmed that the elastic-plastic buckling occurred at the edge portion of the strip through the rolls according to the magnitude of the thickness and the width of the strip. On the basis of the experimental results mentioned above and the theory of the buckling of the plates, the critical condition on the occurrence of edge waves in the forming of the circular channel section with side flanges was obtained.

1. Introduction

In cold roll forming of strip, when the design of roll profiles or the choice of forming conditions is unreasonable, an edge wave occurs at the edge portion of strip. The mechanism of the occurrence of this edge wave has hitherto been considered as a buckling due to compressive residual stresses produced by an unbalanced elongation at the

* Department of Mineral Science and Technology.

** Department of Mineral Science and Technology. Present address: Department of Precision Engineering, Faculty of Engineering, Yamanashi University, Takeda 4-3-11, Kofu 400.

edge portion of the strip during passage through the rolls as compared with the center portion of strip.

In 1967, in Japan, Dr. Murota and Dr. Jimma[1] investigated experimentally the edge wave occurring in forming an aluminum and steel strip into angle sections. They found that the tensile strain at the edge portion of the strip during passage through the rolls was not always large, and they also tried to calculate buckling stresses. In 1973, Kimura[2] investigated some methods to avoid edge waves by means of roll control and of fitting shoes in the forming of an aluminum ceiling.

We have carried out experimental investigations on the deformation process of the strip, the forming load and the forming torque in forming a trapezoidal channel section with side flanges by cold roll forming according to the method of transforming a circular channel section into a trapezoidal channel section since 1963[3~8].

This paper deals with experimental considerations on the mechanism of the occurrence of the edge wave occurring in forming the circular channel sections with side flanges by a single stand roll forming. These considerations are necessary for the preforming of trapezoidal channel sections with side flanges.

2. Roll Profiles and Dimensions of Rolls

Once the edge wave has occurred, it is hardly rectified by subsequent mill rolls. Consequently, to grasp the mechanism of the occurrence of the edge wave precisely, the investigation of single stand roll forming is required.

Firstly, the circular section of the roll profile is determined by five factors, namely, the pass height (h), the opening width of the groove (l), the length measured along the roll profile (S), the transverse bending radii of the groove part and the shoulder part of the roll profile (R) and (r), and the bending angle (θ). Taking the notations as shown in Fig. 1, the following three expressions can be obtained for the convex (upper) roll profile.

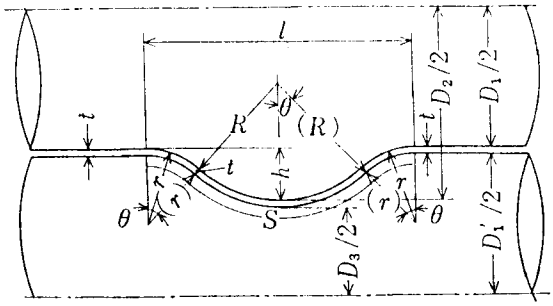

Fig. 1. Notations of the roll profile.

$$\left.\begin{aligned}(R+r)(1-\cos\theta)&=h\\2(R+r)\theta&=S(=77\text{ mm})\\2(R+r)\sin\theta&=l\end{aligned}\right\}\qquad(1)$$

Secondly, the convex roll profiles and dimensions of the two sets of mill rolls used for this experiment are shown in Fig. 2 and Table 1 respectively. To avoid breaking the lead wires of the resistance strain gauges on the strip, several grooves (8 mm in width, 5 mm in depth) were cut in each position on these rolls coinciding with the strain measuring positions on the strip.

The dimensions of the strip SPC-1 (JIS·G3310) used in this experiment are 1 m～2 m in longitudinal length, 94 mm～200 mm in width and 0.4 mm～2.0 mm in thickness. The stress-strain relation of the strip, 1 mm in thickness, mainly used in stress analyses, is shown in Fig. 3.

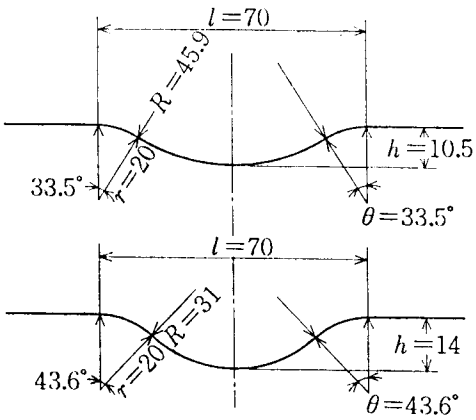

Fig. 2. Geometries of the convex roll profiles used for the experiment.

Table 1. Dimensions of rolls and roll profiles.

Length measured along the roll profile S [mm]	Barrel diam. of male roll D_1 [mm]	Max. diam. of male top roll D_2 [mm]	Barrel diam. of female roll D'_1 [mm]	Min. diam. of female bottom roll D_3 [mm]
77	110	131	110	78
77	110	138	110	78
Ratio of roll diams. $i=D_2/D_3$	Pass height h [mm]	Opening width of groove l [mm]	Forming ratio h/l	
1.68	10.5	70	0.15	
1.77	14	70	0.2	

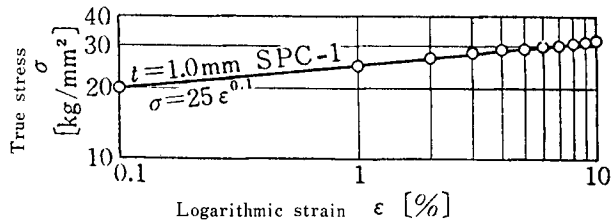

Fig. 3. Stress-strain curve of the strip mainly used for the experiment.

In this experiment, the rolling velocity of the strip was about 30 meters a minute and a lubricant was not used.

The notations used in this paper are as follows.

t, b Strip thickness and width

α Entry angle of the strip $\alpha=\tan^{-1}(H/L)$, where:

L=Distance between the guide and mill rolls

H=Height difference between the biting parts of the flat rolls in the guide and the mill

α is positive when the guide rolls are higher than the mill rolls.

$R.C$ Roll clearance, in this experiment R.C=t

i Ratio of maximum convex to minimum concave roll diameters

h Pass height

l Opening width of groove

S Length measured along the roll profile

h/l Ratio of pass height to opening width of groove, in short, forming ratio

E, ν, σ_e, H' Modulus of elasticity in tension and compression, Poisson's ratio, yield stress, and modulus of work-hardening of the strip, respectively

x, y, z Rectangular coordinates, i. e., transverse distance along the roll profile from the center of the circular channel section, longitudinal distance from the center of mill rolls, and thickness direction of the strip, repectively

ε_{mx}, ε_{my}, ε_{mz} Membrane strains in x, y, and z directions

γ_{mxy} Shearing strain in the xy plane

σ_{mx}, σ_{my}, σ_{mz} Membrane stresses in x, y, and z directions

τ_{mxy} Shearing stress in the xy plane

σ'_{mx}, σ'_{my}, σ'_{mz} Deviatoric components of membrane stresses in x, y, and z directions

$\bar{\varepsilon}_m$, $\bar{\sigma}_m$ Equivalent membrane strain and corresponding membrane stress

ε_m, σ_m Longitudinal residual membrane strain and corresponding membrane stress

σ_{My} Maximum value of the longitudinal compressive membrane stress at the edge portion of strip

ξ Nondimensional transverse position on the side flange, $\xi=\left(x-\frac{S}{2}\right)/\left(\frac{b}{2}-\frac{S}{2}\right)$

A, B Amplitude and span of the edge wave

3. Calculating Equations for Stress Analyses

We have hitherto experimentally observed that the occurrence of the edge wave could not be estimated from only the magnitude of the deflection occurring at the edge portion of the strip at the entrance of the rolls during formation. Therefore, we paid attention to the elongation and the contraction, that is, the membrane starins produced at each point of the strip during passage through the rolls. We thereby obtained the transitions of the membrane stresses from those of the membrane starins, helpful for considering the mechanism of the occurrence of the edge wave.

In calculating the membrane stresses, since we set the roll clearance equal to the strip thickness in this experiment, we assumed both the plane strain in the strip plane (in the xy plane) and the stress=0 in thickness direction (in z direction), and also neglected the Bauschinger effect. Further, the material was assumed to be homogeneous and isotropic.

Firstly, in elastic and unloading processes, the following Hooke equation was used.

$$\begin{Bmatrix} d\sigma_{mx} \\ d\sigma_{my} \\ d\tau_{mxy} \end{Bmatrix}=\frac{E}{1-\nu^2}\begin{bmatrix} 1 & \nu & 0 \\ \nu & 1 & 0 \\ 0 & 0 & (1-\nu)/2 \end{bmatrix}\begin{Bmatrix} d\varepsilon_{mx} \\ d\varepsilon_{my} \\ d\gamma_{mxy} \end{Bmatrix} \tag{2}$$

Secondly, in the plastic loading process, the following adversely transformed equation[9] reduced by Dr. Yamada to the Reuss equation was used.

$$\begin{Bmatrix} d\sigma_{mx} \\ d\sigma_{my} \\ d\tau_{mxy} \end{Bmatrix}=\frac{E}{Q}\cdot$$

$$\begin{bmatrix} \sigma'^{2}_{my}+2P & -\sigma'_{mx}\sigma'_{my}+2\nu P & -\frac{\sigma'_{mx}+\nu\sigma'_{my}}{1+\nu}\tau_{mxy} \\ -\sigma'_{mx}\sigma'_{my}+2\nu P & \sigma'^{2}_{mx}+2P & -\frac{\sigma'_{mx}+\nu\sigma'_{my}}{1+\nu}\tau_{mxy} \\ -\frac{\sigma'_{mx}+\nu\sigma'_{my}}{1+\nu}\tau_{mxy} & -\frac{\sigma'_{my}+\nu\sigma'_{mx}}{1+\nu}\tau_{mxy} & \frac{R}{2(1+\nu)}+\frac{2H'}{9E}(1-\nu)\bar{\sigma}_m^2 \end{bmatrix}\begin{Bmatrix} d\varepsilon_{mx} \\ d\varepsilon_{my} \\ d\gamma_{mxy} \end{Bmatrix} \tag{3}$$

where

$$P=\frac{2H'}{9E}\bar{\sigma}_m{}^2+\frac{\tau_{mxy}{}^2}{1+\nu},\quad Q=R+2(1-\nu^2)P,\quad R=\sigma'_{mx}{}^2+2\nu\sigma'_{mx}\sigma'_{my}+\sigma'_{my}{}^2$$

$$\bar{\sigma}_m{}^2=\frac{3}{2}(\sigma'_{mx}{}^2+\sigma'_{my}{}^2+\sigma'_{mz}{}^2+2\tau'_{mxy}{}^2),\quad \sigma'_{mx}=(2\sigma_{mx}-\sigma_{my})/3$$

$$\sigma'_{my}=(2\sigma_{my}-\sigma_{mx})/3,\quad \sigma'_{mz}=(-\sigma_{mx}-\sigma_{my})/3,\quad \tau'_{myz}=\tau_{myz}=0$$

$$\tau'_{mzx}=\tau_{mzx}=0,\quad \tau'_{mxy}=\tau_{mxy}$$

Denoting by f the plastic potential, the decision of unloading was based on the relation $df=(\partial f/\partial\sigma_{ij})d\sigma_{ij}<0$. Besides, the mechanical properties of the strip were taken as $\sigma_e=20$ kg/mm^2, $E=2.1\times10^4$ kg/mm^2, $H'=471$ kg/mm^2, $\nu=0.3$ or 0.5 in elastic or plastic region respectively, by idealizing the stress-strain relation shown in Fig. 3 as the linear work-hardening type.

4. Relations between Forming Conditions, Membrane Strains, and Membrane Stresses

4.1 Effect of the entry angle of the strip on membrane strains and corresponding membrane stresses

Firstly, a typical example of the edge wave occurring on the exit side of the rolls is shown in Fig. 4. The magnitude of the edge wave is represented by the amplitude A [mm] and the span B [mm], as shown in Fig. 5.

Figures 6 and 7 show the relations between the entry angle (α) of the strip to the rolling axis and the amplitude (A), and the span (B) of the edge wave, where $S=77$ mm,

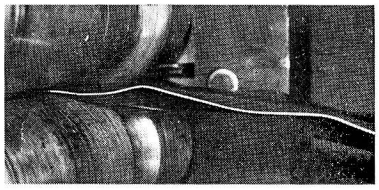

Fig. 4. A photograph showing an example of the edge wave occurring at the exit of rolls.

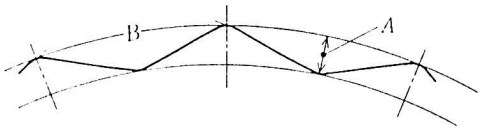

Fig. 5. Presentation of the magnitude of the edge wave of the product.

h/l=0.2, b/S=2.6, t=1.0 mm and i=1.77. Under this condition, the edge wave began to occur for $\alpha \cong -2°$. From Fig. 6, it is found that the amplitude of the edge wave increases approximately proportionally to the entry angle for $-2° \leq \alpha \leq 6°$. Further, from Fig. 7, it is found that the span of the edge wave increases slightly with an increase in the positive entry angle for $0° \leq \alpha \leq 6°$. On the other hand, in the case of the negative entry angle, the span increases abruptly with an increase in the absolute value of the entry angle for $-2° \leq \alpha \leq 0°$, and becomes infinity for $\alpha = -2°$. Namely, the edge wave grows in intensity with the positive large entry angle, that is, with the large entrly angle on the convex roll side.

Secondly, the membrane strains produced during passage through the rolls were

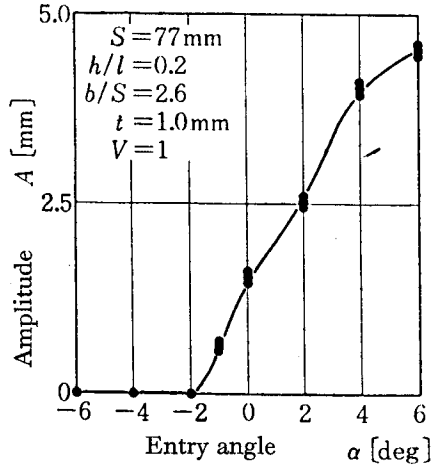

Fig. 6. Effect of the entry angle (α) of the strip on the amplitude (A) of the edge wave of the product.

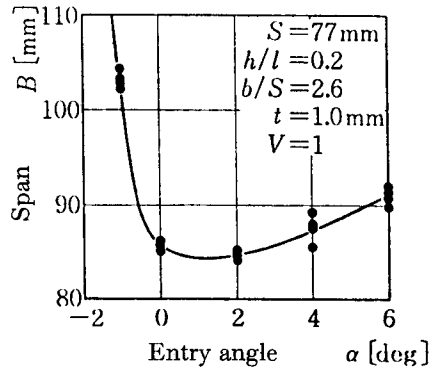

Fig. 7. Effect of the entry angle (α) of the strip on the span (B) of the edge wave of the product.

measured by resistance strain gauges on the strip under the same conditions as mentioned above, and the corresponding membrane stresses were calculated form Eqs. (2) and (3) by using the measured membrane strains.

Figures 8 and 9 show the transitions of the transverse membrane strains (ε_{mx}) and the longitudinal membrane starins (ε_{my}) produced at the center (x=0 mm) of the circular channel section, with the distance (y) from the center of the rolls, taking the entry angle of the strip for the parameter, where h/l=0.2, b/S=2.6 and t=1.0 mm. In these figures, the dotted line represents the transition of the membrane strain in the case where the edge wave occurred. On the other hand, the solid line represents the same in the absence of the edge wave. From these figures, it is found that the longitudinal membrane strain at the center of the circular channel section is tensile at the entrance of the rolls, and com-

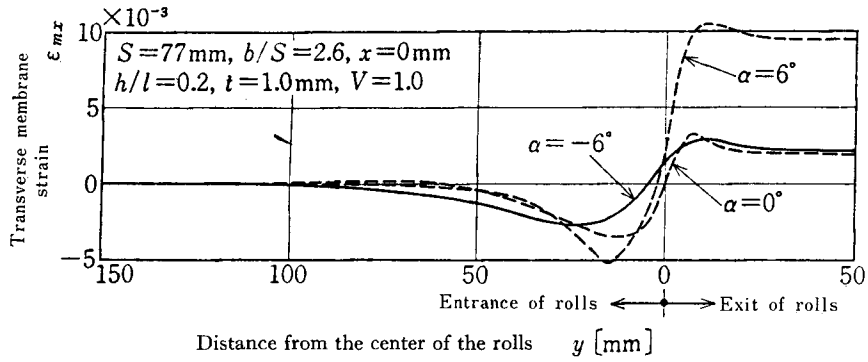

Fig. 8. Transition of the transverse membrane strains (ε_{mx}) occurring at the center (x=0 mm) of the circular channel section during passage through the rolls in the case of h/l=0.2, b/S=2.6 and t=1.0 mm (Solid line: No edge wave occurred, Dotted line: The edge wave occurred).

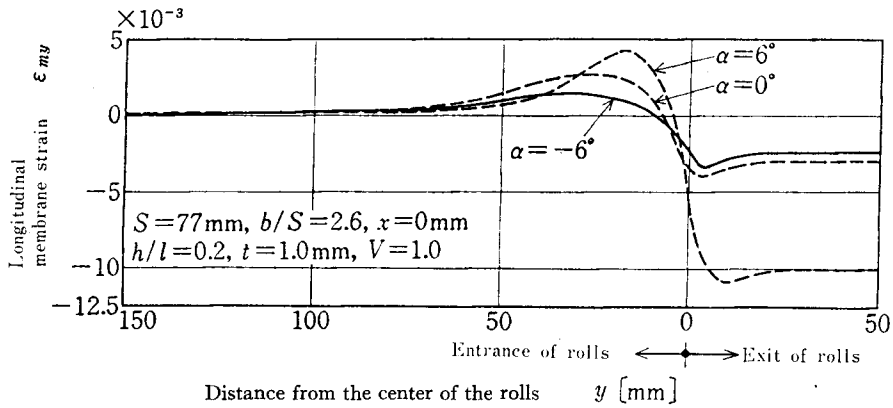

Fig. 9. Transition of the longitudinal membrane strains (ε_{my}) (x=0 mm, h/l=0.2, b/S=2.6, t=1.0 mm).

pressive at the exit of the rolls, regardless of the entry angle. On the other hand, the transverse membrane starin is opposite to the longitudinal one. Namely, the product after roll forming is contarcted longitudinally, and elongated transversely, at the center of the circular channel section. Also the magnitudes of these strains, in the case where the edge wave occurred, are larger than those in the absence of the edge wave.

Further, from the observation of the transitions of the longitudinal membrane strains and the corresponding membrane stresses in the side flange, it is thought that the difference between them, in the two cases where the edge wave occurred and did not, becomes clearer in comparison with them at the center of the circular channel section..

Figures 10(a), 10(b) and 10(c) show the transverse distributions and their transitions of the longitudinal membrane stresses (σ_{my}), together with the transverse distributions of the longitudinal residual membrane strains (ε_m) in the side flange, in the case of $\alpha=6°$, $0°$ and $-6°$, where $h/l=0.2$, $b/S=2.6$ and $t=1.0$ mm. Here, each transverse position on the side flange is denoted by $\xi=(x-S/2)/(b/2-S/2)$. In these figures, each line which shows the distance from the center of the rolls gives the zero-line of the stress in each position, and the tensile or the compressive stress is shown on the upper or the lower side of this line respectively. From these figures, it is found that the compressive stress

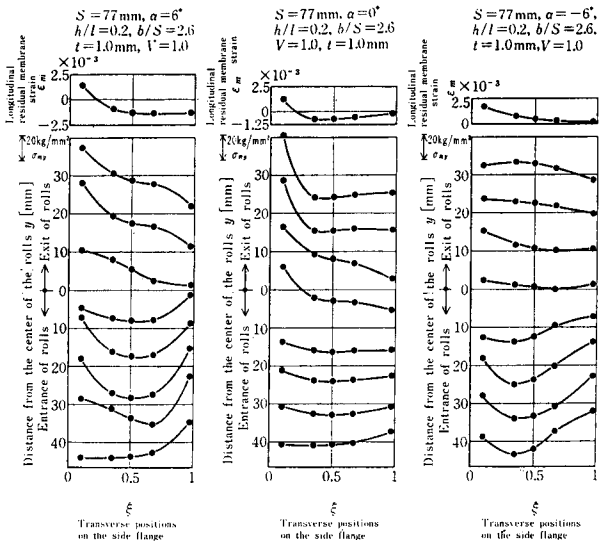

Fig. 10. The longitudinal residual membrane strains (ε_m) and both the distributions and their transitions of the longitudinal membrane stresses (σ_{my}) in the side flange ($h/l=0.2$, $b/S=2.6$, $t=1.0$ mm).

(a): Entry angle $\alpha=6°$
(b): $\alpha=0°$ } The edge wave occurred.
(c): $\alpha=-6°$ No edge wave occurred.

and strain prevail in the transverse distributions of both the longitudinal membrane stress at the exit of the rolls and the longitudinal residual membrane strain, in the case of $\alpha=0°$ and 6° where the edge wave occurred. On the other hand, in the case of $\alpha=-6°$ where the edge wave did not occur, the tensile stress and strain prevail. This tendency was also observed for $b/S=2.08$.

Under the same conditions as shown in Fig. 10, the transitions of the longitudinal membrane strain (ε_{my}) and the corresponding stress (σ_{my}) at the edge portion ($x=98$ mm, $\xi=0.97$) of the side flange are shown in Figs. 11 and 12 respectively, with the distance (y) from the center of the rolls, taking the entry angle (α) for the parameter. In these figures, the dotted line represents the transitions in the case where the edge wave occurred, and the solid line, on the other hand, shows the transitions in the absence of the edge wave. From these figures, it is found that both the longitudinal membrane strain and the corresponding stress change from tension into compression, but they do not change abruptly in the case of $\alpha=-6°$ where the edge wave did not occur. On the other hand, in the case of $\alpha=0°$ and 6° where the edge wave occurred, there are maximum values of the compressive strain and stress at the exit position about 10 mm from the cnter of the rolls. The relation between the maximum value (σ_{My}) of the longitudinal compressive membrane stress at the edge portion ($x=98$ mm, $\xi=0.97$) of the side flange and

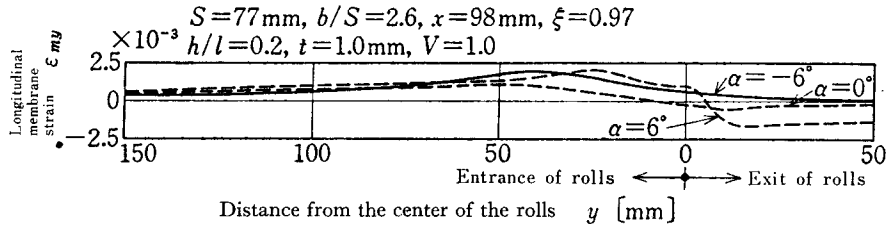

Fig. 11. Transition of the longitudinal membrane strains (ε_{my}) ($\xi=0.97$, $h/l=0.2$, $b/S=2.6$, $t=1.0$ mm, Solid line: No edge wave occurred, Dotted line: The edge wave occurred).

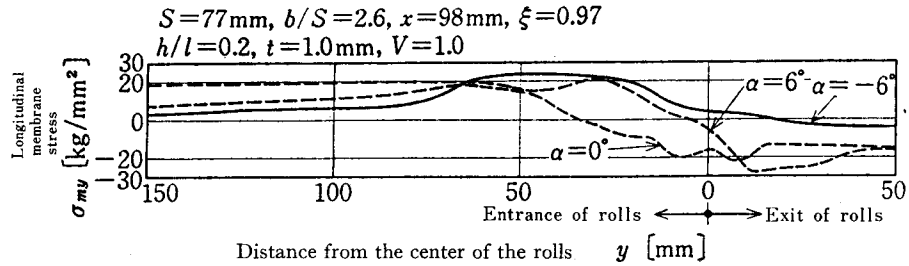

Fig. 12. Transition of the longitudinal membrane stresses (σ_{my}) ($\xi=0.97$, $h/l=0.2$, $b/S=2.6$, $t=1.0$ mm, Solid line: No edge wave occurred, Dotted line: The edge wave occurred).

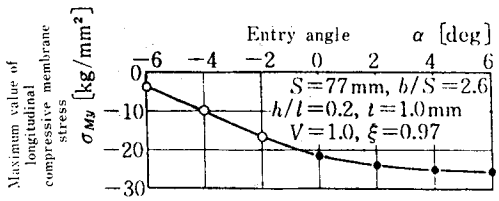

Fig. 13. Effect of the entry angle (α) of the strip of the maximum value (σ_{My}) of the longitudinal compressive membrane stress (ξ=0.97, h/l=0.2, b/S=2.6, t= 1.0 mm, ○: No edge wave occurred, ●: The edge wave occurred).

the entry angle (α) of the strip is shown in Fig. 13, where h/l=0.2, b/S=2.6 and t=1.0 mm. From this figure ,it is found that the maximum value σ_{My} increases abruptly with a change from the negative into the positive entrly angle, and becomes $|\sigma_{My}| \geq 20$ kg/mm² for $\alpha \geq -1°$. However, the ratio of this increase becomes quite small for $\alpha \geq 2°$.

4.2 Effect of the ratio of pass height to opening width of circular groove on membrane strains and corresponding membrane stresses

Since the edge wave once occurred is hardly rectified by subsequent mill rolls, the design of the roll profile in the first mill rolls, excluding pinch rolls, is very important. Here, we examined the effect of the pass height on the membrane strains and the corresponding membrane stresses produced during passage through the rolls under the conditions h/l=0.15, b/S=2.6, t=1.0 mm and α=0°. This is because the edge wave occurred under the conditions h/l=0.2, b/S=2.6, t=1.0 mm and α=0° as shown in 4.1.

Figure 14 shows the transitions of both the transverse membrane strain (ε_{mx}) and the longitudinal membrane strain (ε_{my}) at the center (x=0 mm) of the circular channel section, with the distance (y) from the center of the rolls. In this figure, the broken line represents the transverse membrane strain, and the solid line, on the other hand, represents the longitudinal membrane strain. As seen in this figure, the tendency of these transitions is quite similar to that in the case where h/l=0.2 and α=0°, as shown in Figs. 8 and 9. However, these latter values are smaller than the former.

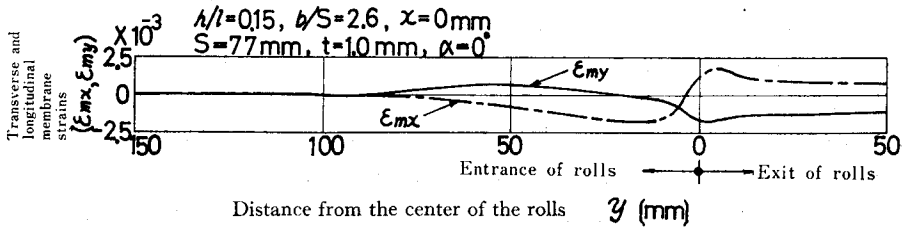

Fig. 14. Transition of both the transverse and the longitudinal membrane strains (ε_{mx}, ε_{my}) (x=0 mm, h/l=0.15, α=0°, b/S=2.6, t=1.0 mm, Broken line: The transverse membrane strain ε_{mx}, Solid line: The longitudinal membrane strain ε_{my}).

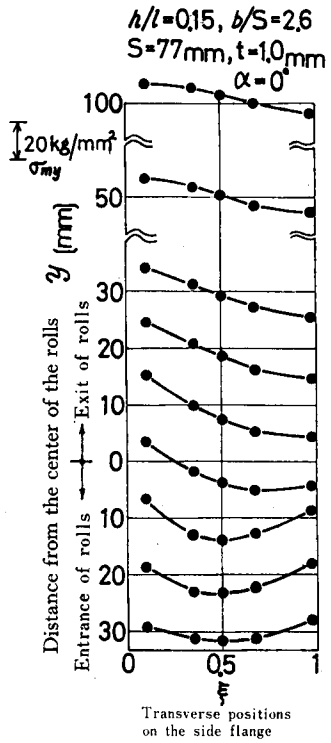

Fig. 15. Distributions and their transitions of the longitudinal membranes sresses (σ_{my}) in the side flange (h/l=0.15, α=0°, b/S=2.6, t=1.0 mm).

Next, the transverse distribution and its transition of the longitudinal membrane stress (σ_{my}) in the side flange are shown in Fig. 15, with the distance (y) from the center of the rolls. In this figure, each line shows the distance from the center of the rolls gives the zero-line of the stress in each position. The tensile or the compressive stress is shown on the upper or the lower side of this line respectively. From this figure, it is found that the transverse distribution zone of the longitudinal tensile membrane stress increases gradually at the exit of the rolls, and at last, becomes dominant in the residual membrane stress distribution at the exit position y=100 mm. It is also found that this tendency is similar to that in the case of h/l=0.2 and α=−6°, as shown in Fig. 10(c).

Under the same condition as shown in Fig. 15, the transitions of the longitudinal membrane strain (ε_{my}) and the corresponding membrane stress (σ_{my}) at the edge portion (x=98 mm, ξ=0.97) of the side flange are shown in Figs. 16(a) and 16(b) respectively. As seen in these figures, the tendency of these transitions is similar to that in the case where h/l=0.2 and α=0°, as shown in Figs. 11 and 12. However, these latter values are smaller than the former.

Figures 17(a) and 17(b) show the transverse distributions of the longitudinal residual

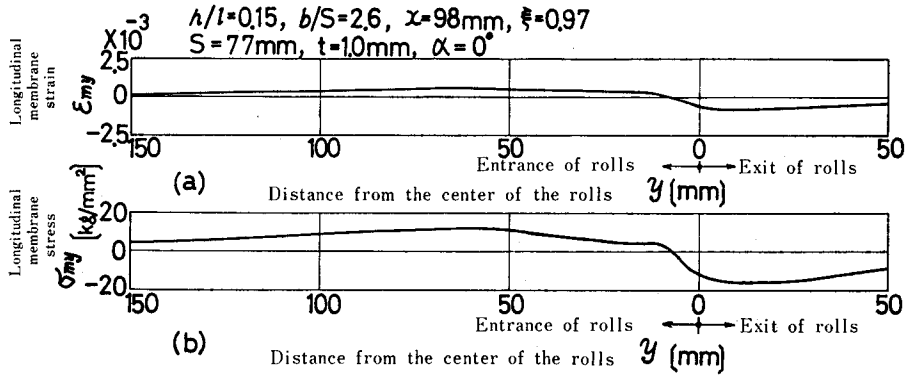

Fig. 16. Transitions of both the longitudinal membrane strain (ε_{my}) and the corresponding membrane stress (σ_{my}) (ξ=0.97, h/l=0.15, α=0°, b/S=2.6, t=1.0 mm).

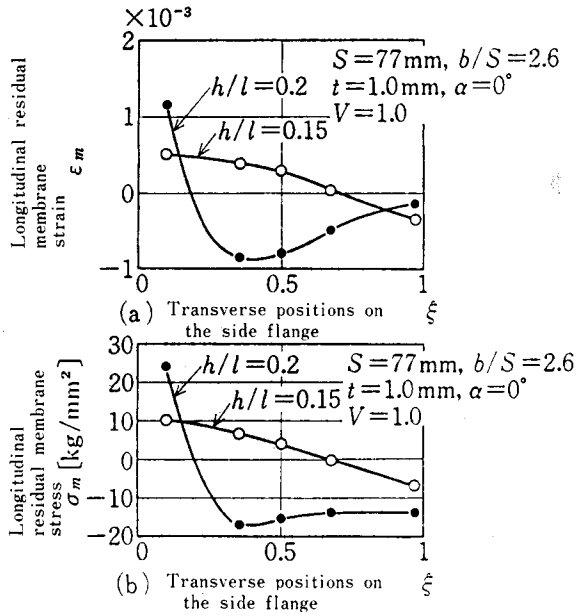

Fig. 17. Distributions of both the longitudinal residual membrane strain (ε_m) and the corresponding residual membrane stress (σ_m) in the side flange (h/l=0.15, 0.2).

membrane strain (ε_m) and the corresponding residual membrane stress (σ_m) in the side flange in the case of h/l=0.15 and h/l=0.2, where b/S=2.6, t=1.0 mm and α=0°. As seen in these figures, the longitudinal residual membrane strain and the corresponding residual membrane stress are tensile at the shoulder portion, and compressive at the edge portion in both cases. In the middle point of the flnge, on the other hand, they are tensile

for $h/l=0.15$, that is, in the absence of the edge wave, and compressive for $h/l=0.2$, that is, in the presence of the edge wave.

4.3 Effect of the strip thickness and width on membrane strains and Corresponding membrane stresses

Among several factors which affect the occurrence of the edge wave, the magnitude of the strip thickness and width is an important factor. Figure 18 shows the effect of both the strip thickness (t) and the ratio (b/S) of the strip width to the length measured along the roll profile on the occurrence of the edge wave, under the conditions $h/l=0.2$ and $\alpha=0°$. In this figure, symbol ● represents the case where the edge wave occurred, and symbol ○, on the other hand, represents the case where the edge wave did not occur. As seen in this figure, in genreal, the edge wave is apt to occur for thin and wide strips.

Next, the relations between the maximum value (σ_{My}) of the longitudinal compressive membrane stress at the edge portion ($\xi=0.97$) of the side flange and the strip

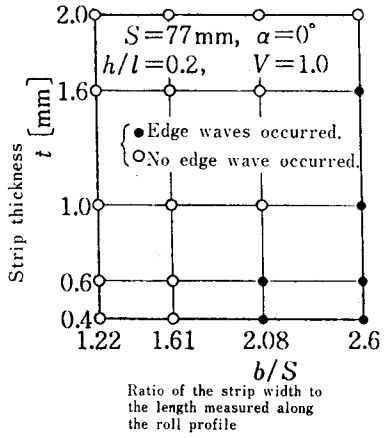

Fig. 18. Effect of both the strip thickness (t) and the ratio (b/S) of the strip width to the length measured along the roll profile on the occurrence of the edge wave ($h/l=0.2$, $\alpha=0°$, ○: No edge wave occurred, ●: The edge wave occurred).

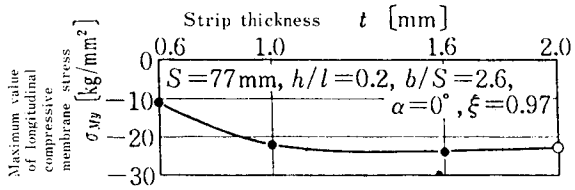

Fig. 19. Effect of the strip thickness (t) on the maximum value (σ_{My}) of the longitudinal compressive membrane stress ($\xi=0.97$, $h/l=0.2$, $\alpha=0°$, $b/S=2.6$, ●: The edge wave occurred, ○: No edge wave occurred).

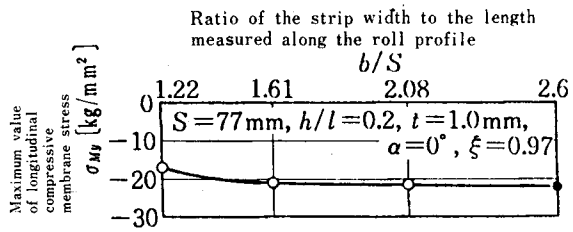

Fig. 20. Effect of the ratio (b/S) of the strip width to the length measured along the roll profile on the maximum value (σ_{My}) of the longitudinal compressive membrane stfress ($\xi=0.97$, $h/l=0.2$, $\alpha=0°$, $t=1.0$ mm, ○: No edge wave occurred, ●: The edge wave occurred).

thickness (t), and the ratio (b/S) of the strip width to the length measured along the roll profile are shown in Figs. 19 and 20, respectively. In these figures, symbols ● and ○ coincide with those in Fig. 18. From these figures, it is found that the absolute value of σ_{My} increases with an increase in both the strip thickness (t) and the ratio (b/S), and mostly becomes $|\sigma_{My}| \geq 20$ kg/,mm². However, in these relations, the difference is not clear between the stress values in both cases.

Next, we examined the residual membrane strain in the side flange of the product. Figure 21 shows the transverse distribution of the longitudinal residual membrane strain

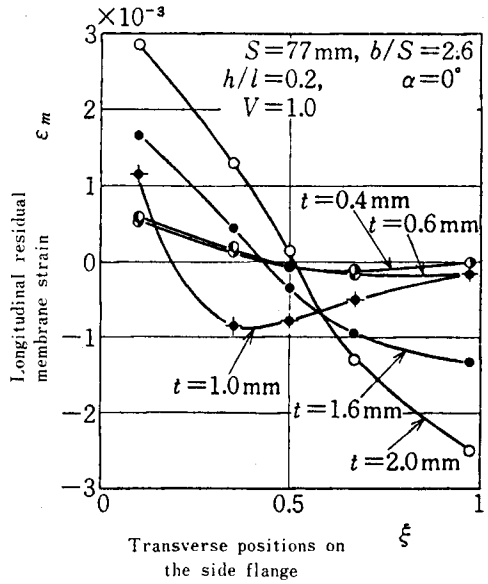

Fig. 21. Effect of the strip thickness (t) on the distribution of the longitudinal residual membrane strain (ε_m) in the side flange ($h/l=0.2$, $\alpha=0°$, $b/S=2.6$, ○: No edge wave occurred, Other symbols: The edge wave occurred).

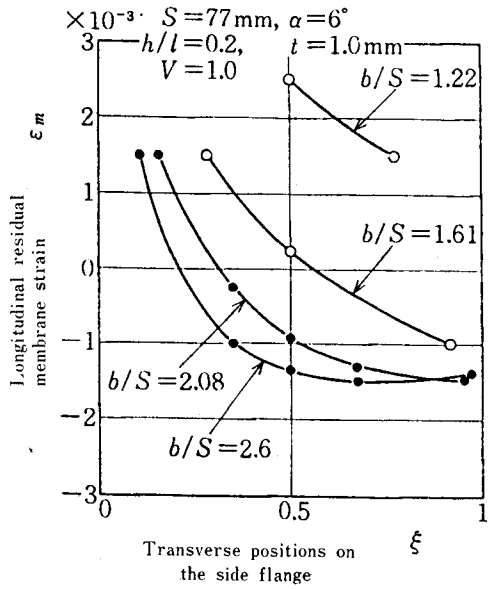

Fig. 22. Effect of the ratio (b/S) of the strip width to the length measured along the roll profile on the distribution of the longitudinal residual membrane strain (ε_m) in the side flange ($h/l=0.2$, $\alpha=6°$, $t=1.0$ mm, ○: No edge wave occurred, ●: The edge wave occurred).

(ε_m) in the flange for different strip thicknesses, under the constant strip width $b/S=2.6$. In this experiment, as shown in Fig. 18, the edge wave occurred for $t=0.4$ mm to 1.6 mm, but did not for $t=2.0$ mm. As seen in this figure, the longitudinal residual membrane strain is tesnile or compressive at the shoulder portion or at the edge portion respectively, and the absolute values of these strains increase with an increase in the strip thickenss.

On the other hand, at the middle portion of the flange, it is not necessarily so. Namely, only the longitudinal residual membrane strain for $t=2.0$ mm in the absence of the edge wave is positive, that is, tensile at the middle point ($\xi=0.5$) of the flange. This tendency is also observed for different strip widths. Figure 22 shows the transverse distribution of the longitudinal residual membrane strain (ε_m) in the flange, in the case where $h/l=0.2$, $t=1.0$ mm and $\alpha=6°$, taking the ratio (b/S) for the parameter. In this experiment, the edge wave occurred for $b/S=2.08$ and 2.6, but did not for $b/S=1.22$ and 1.61. From this figure, it is found that the value of the longitudinal residual membrane strain at the middle point ($\xi=0.5$) of the flange becomes positive, that is, tensile, as the strip width becomes narrower under the constant strip thickness.

5. Critical Conditions for the Occurrence of Edge Waves

From the experimental results shown before, it was found that the product after roll forming was contracted longitudinally at the center ($x=0$ mm) of the circular channel

section, and elongated at the shoulder portion, and had both conditions (contraction, elongation) at the edge portion of the side flange according to the magnitude of the strip and to the entry angle. It was also found that from the transevrse distribution form of the longitudinal residual membrane strain in the flange, the value of this membrane strain at the middle point ($\xi=0.5$) of the flange was positive (elongation) in the absence of the edge wave, and negative (contraction) in the presence of the edge wave.

Then ,we examined the relation between the longitudinal contraction at the center ($x=0$ mm) of the circular channel section during passage through the rolls and the longitudinal residual membrane strain in the flange. This relation is shown in Fig. 23, in which $\varepsilon_{m\xi}$ is plotted against ε_{Mg}. Here, $\varepsilon_{m\xi}$ represents the longitudinal residual membrane strain at the middle point ($\xi=0.5$) of the flange, and ε_{Mg} represents the maximum value of the longitudinal compressive membrane strain at the center ($x=0$ mm) of the circular channel section. Also, symbol ● represents the case where the edge wave occurred, and symbol ○, on the other hand, represents the case where the edge wave did not occur. From this figure, it is found that though the correlation between ε_{Mg} and $\varepsilon_{m\xi}$ is not always clear, the values of $\varepsilon_{m\xi}$ become negative for $|\varepsilon_{Mg}|\geq 4\times10^{-3}$ and at the same time the edge wave occurs without fail, excluding such thin strips as $t=0.4$ mm and 0.6 mm corresponding with the two black points for $|\varepsilon_{Mg}|\leq 2\times10^{-3}$. It is also thought that this gives a qualitative explanation for the phenomenon observed in production fields where the edge wave hardly occurs in the forming of the strip which was elongated longitudinally at the middle portion in hot or cold rolling.

Next, we paid attention to the maximum value (σ_{My}) in the absolute value of the

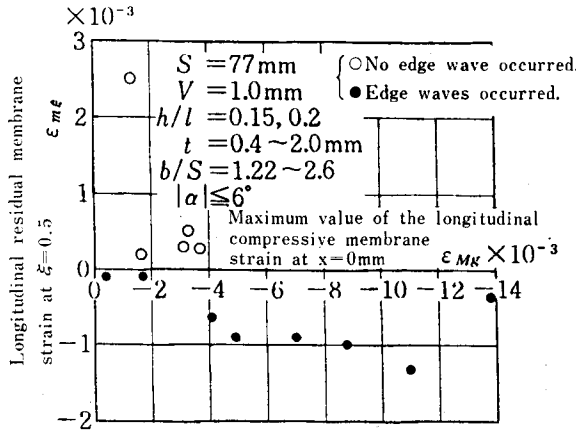

Fig. 23. Relation between the maximum value (ε_{Mg}) of the longitudinal compressive membrane strain at $x=0$ mm and the longitudinal residual membrane strain ($\varepsilon_{m\xi}$) at $\xi=0.5$ (○: No edge wave occurred, ●: The edge wave occurred).

longitudinal compressive membrane stress at the edge portion ($\xi=0.97$) of the flange during passage through the rolls, and discussed the mechanism of the occurrence of the edge wave from the aspect of the buckling. The compressive stress (σ_{cr}) of the buckling of the plate, in general, is given by the following equation.

$$\sigma_{cr}=k\cdot\frac{E_t}{E}\cdot\frac{\pi^2E}{12(1-\nu^2)}\cdot\left(\frac{t}{b'}\right)^2 \tag{4}$$

where,

k=a factor which is determined by both the ratio of the magnitude (B') of a wave length to the plate width (b') and the restricting conditions at the edge of the plate

$E_t=d\sigma/d\varepsilon$, in the elastic behavior $E_t/E=1$

For each forming condition, the relation is shown in Fig. 24, namely between the ratio (σ_{My}/σ_e) of the maximum value (σ_{My}) of the longitudinal compressive membrane stress at the edge portion ($\xi=0.97$) of the flange to the yield stress (σ_e) of the strip and the term $(\pi^2E/12(1-\nu^2))(t/b')^2$, excluding the factor $(k\cdot E_t/E)$ from the right side of Eq. (4). Here, the buckling plate width b' was taken as $b'=(b-S)/4$, because the transverse distribution zone of the longitudinal compressive membrane stress in the flange ranged from about the middle point of the flange to the edge portion, when the edge wave occurred.

In Fig. 24, the solid line represents the boundary line for the case where the edge wave occurred or did not occur. Also, the symbol ● (for $h/l=0.2$) over this line represents the case where the edge wave occurred, and both symbols ○ (for $h/l=0.2$) and △

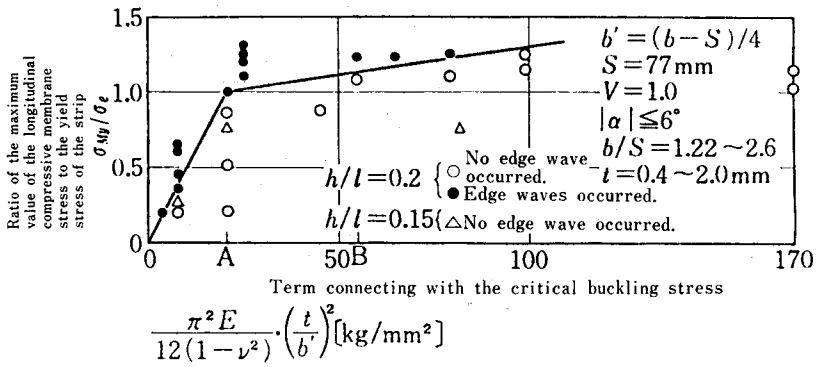

Fig. 24. Relation between the ratio (σ_{My}/σ_e) of the maximum value (σ_{My}) of the longitudinal compressive membrane stress at $\xi=0.97$ to the yield stress (σ_e) of the strip and the term $(\pi^2E/12(1-\nu^2))(t/b')^2$ connecting with the critical buckling stress (○, △: No edge wave occurred, ●: The edge wave occurred).

(for $h/l=0.15$) under this line represent the cases where the edge wave did not occur. As seen in this figure, the edge wave occurs for the compressive stress less than the compressive yield stress $\sigma_e=20$ kg/mm^2 of the strip within the range from the origin to the position A in the axis of abscissa. Consequently, the occurrence of the edge wave in this case is considered to be due to the elastic buckling, and for thin and wide strips, the buckling or the edge wave occurs easily according to the samll compressive stress. Thus, in this case, the forming ratio (h/l) or the pass height must be taken as $h/l=0.15$, as shown in Fig. 24. Besides, in this experiment, the value of k was about 1.0 from the inclination of the boundary line within this range.

Further, in the case beyond the position A in the axis of abscissa, that is, for thick and narrow strips, the edge wave occurs for the compressive stress more than the compressive yield stress, and this is considered to be due to the so-called plastic buckling. However, the value of the ratio σ_{My}/σ_e increases with an increase in the ratio (t/b'), but only slightly.

In either case, from Fig. 24, it is found from the experimental results that, in the case of $h/l=0.2$ and the standard pass line $\alpha=0°$, the edge wave did not occur on the right side beyond the position B in the axis of abscissa, that is, for $(\pi^2E/12(1-\nu^2))(t/b')^2\geq 55$, the product without the edge wave in a single stand roll forming can be expected for the strip which satisfies the relation $t/(b-S)\geq 1.222\times 10^{-2}$, but for the strip which does not satisfy this relation, the forming ratio or the pass height must be taken as $h/l=0.15$.

6. Conclusion

We discussed the mechanism of the occurrence of the edge wave occurring in forming the strip into a circular channel section with side flanges by a single stand roll forming, from the relations between the forming conditions and the membrane strains, and the corresponding membrane stresses calculated from these strains produced during passage through the rolls, and we obtained the following results.

(1) The longitudinal component of the finished product is contracted at the center of the circular channel section, and elongated at the shoulder portion, and has both conditions (contraction, elongation) at the edge portion according to the forming conditions. In the absence of edge waves, the transverse distribution zone of both the positive longitudinal residual membrane strain and the corresponding membrane stress ranges from the shoulder portion to beyond the middle point of the flange.

(2) The correlation is observed to a certain extent between the magnitude of the contraction at the center of the circular channel section and the elongation, and the contraction at the middle portion of the flange. In this experiment, when the maximum value

of the longitudinal compressive membrane strain at the center of the circular channel section was over 0.4%, edge waves occurred for the strip thickness over 0.8 mm without fail.

(3) The occurrence of edge waves is considered to be due to the elastic-plastic buckling occurrirng at the edge portion of the strip during passage through the rolls according to the magnitude of the strip thickness and width.

(4) In the standard pass line, when the relation $t/(b-S)\geq 1.222\times 10^{-2}$ is satisfied among the strip thickness (t), width (b) and the length (S) measured along the roll profile, the single stand roll forming of the circular channel section with side flanges can be done without the edge wave occurring by taking the forming ratio or pass height as $h/l=0.2$. However, for the strip which does not satisfy this relation, the forming ratio must be reduced, as $h/l=0.15$. In either case, the edge wave hardly occurs for the thick strip, but since the longitudinal curvature, on the other hand, increases, the forming ratio or pass height in the first mill rolls, excluding pinch rolls, should be taken as about $h/l=0.15$ in the forming of the circular channel section with side flanges, if both the edge wave and the longitudinal curvature are taken into consideration.

Acknowledgement

We are grateful for the financial assistance of the Ministry of Education.

References

1) T. Murota, T. Jimma, I. Kondo and S. Murakami: 18th Meeting of Japan Society for Technology of Plasticity, (Nov. 1967), p. 317.
2) H. Kimura: Meeting of Jap. Soc. for Technol. of Plast., (May 1973), p. 333.
3) J. Kokado and Y. Onoda: Journal of Jap. Soc. for Technol. of Plast., Vol. 13, No. 132, (Jan. 1972), p. 21.
4) J. Kokado and Y. Onoda: ibid., Vol. 13, No. 142, (nov. 1972), p. 851.
5) J. Kokado and Y. Onoda: ibid., Vol. 14, No. 151, (Aug. 1973), p. 612.
6) J. Kokado and Y. Onoda: Memoirs of the Faculty of Engng., Kyoto Univ., Vol. 36, Part 4, (Apr. 1975), p. 443.
7) J. Kokado and Y. Onoda: ibid., Vol. 37, Part 2, (Jan. 1975), p. 10.
8) J. Kokado and Y. Onoda: J. of Jap. Soc. for Technol. of Plast., Vol. 17, No. 181, (Feb. 1976), p. 92.
9) Y. Yamada: ibid., Vol. 10, No. 104, (Sep. 1969), p. 692.